Cell Biol Toxicol (2024) 40:95
https://doi.org/10.1007/s10565-024-09944-8

RESEARCH

METTL14 regulates inflammation in ulcerative colitis via the lncRNA DHRS4-AS1/miR-206/A3AR axis

Weiyun Wu · Xiaowen Li · Zhuliang Zhou · Huanjin He · Cheng Pang · Shicai Ye · Juan-Hua Quan

Received: 20 July 2024 / Accepted: 4 November 2024

Abstract As a chronic inflammatory bowel disease, the pathogenesis of ulcerative colitis (UC) has not been fully elucidated. N6-methyladenosine (m6A) modification, observed in various RNAs, is implicated in inflammatory bowel diseases. Methyltransferase-like 14 (METTL14) is the major subunit of the methyltransferase complex catalyzing m6A modifications. Here, we designated to examine the regulatory effects and mechanisms of METTL14 on long non-coding RNA (lncRNA) during UC progression. METTL14 knockdown decreased cell viability, promoted apoptosis, increased cleaved PARP and cleaved Caspase-3 levels, while reducing Bcl-2 levels. METTL14 knockdown also led to a significant increase in NF-κB pathway activation and inflammatory cytokine production in the Caco-2 cells treated with TNF-α. Moreover, the suppression of METTL14 aggravated colonic damage and inflammation in our dextran sulfate sodium (DSS)-induced murine colitis model. METTL14 silencing suppressed DHRS4-AS1 expression by reducing the m6A modification of *DHRS4-AS1* transcripts. Furthermore, DHRS4-AS1 mitigated inflammatory injury by targeting the miR-206/adenosine A3 receptor (A3AR) axis. DHRS4-AS1 overexpression counteracted the enhancing impact of METTL14 knockdown on TNF-α-induced inflammatory injury in Caco-2 cells. In conclusion, our findings suggest that METTL14 protects against colonic inflammatory injury in UC via regulating the DHRS4-AS1/miR-206/A3AR axis, thus representing a potential therapeutic target for UC.

Keywords Ulcerative colitis · M6A modification · METTL14 · LncRNA DHRS4-AS1 · MiR-206 · A3AR

Abbreviations

UC	Ulcerative colitis
IBD	Inflammatory bowel disease
m6A	N6-methyladenosine
METTL14	Methyltransferase-like 14
3′-UTR	3′ Untranslated region
lncRNA	Long non-coding RNA
miRNA	MicroRNA
TNF-α	Tumor necrosis factor-α
NF-κB	Nuclear factor kappa B

Weiyun Wu and Xiaowen Li are co-first author.

Supplementary Information The online version contains supplementary material available at https://doi.org/10.1007/s10565-024-09944-8.

W. Wu · X. Li · J.-H. Quan (✉)
Laboratory of Gastroenterology, Affiliated Hospital of Guangdong Medical University, Zhanjiang 524001, Guangdong, China
e-mail: quanjuanhua@gdmu.edu.cn

W. Wu · X. Li · Z. Zhou · H. He · C. Pang · S. Ye (✉) · J.-H. Quan
Department of Gastroenterology, Affiliated Hospital of Guangdong Medical University, Zhanjiang 524001, Guangdong, China
e-mail: caizi23@126.com

Published online: 11 November 2024

DAA	3-Deazaadenosine
DSS	Dextran sulfate sodium
DAI	Disease activity index
H&E	Hematoxylin and eosin

Introduction

Inflammatory bowel disease (IBD), featured by non-infectious chronic inflammation of the gastrointestinal tract, encompasses ulcerative colitis (UC), Crohn's disease (CD), and indeterminate colitis (Sairenji et al. 2017). The prevalence of IBD has increased in recent years, thus imposing a considerable burden on society and healthcare systems (GBD 2017 Inflammatory Bowel Disease Collaborators. 2020). Although involvement of genetic changes, immune dysregulation, gut dysbiosis, and environmental influences has been implicated, the specific mechanism inherent IBD pathogenesis remains largely unclarified (Luo et al. 2022). Notably, UC is characterized by the increased levels of inflammatory cytokines, whose expressions are regulated by nuclear factor kappa B (NF-κB); these include interleukin (IL)-1β, IL-6, tumor necrosis factor alpha (TNF-α), and IFN-γ, etc. (Semiz et al. 2020).

Enriched in the 3′ untranslated region (3′-UTR) of transcripts, the N6-methyladenosine (m6A) modification acts as a dynamically reversible post-transcriptional modification. It is found on a variety of RNAs, like microRNAs (miRNAs), long non-coding RNAs (lncRNAs), and messenger RNAs (mRNAs), influencing their metabolism and function (Wang and Lu 2021). m6A modifications are mainly enriched in RRACH motifs (H = A, C, or U; R = G or A) (Luo et al. 2021). Three classes of proteins regulate m6A modifications, acting as "writers", "erasers", and "readers." Methyltransferase-like 3 (METTL3), METTL14, RNA-binding motif protein15 (RBM15), Wilms' tumor 1-associated protein (WTAP), and KIAA1429 are methyltransferases that catalyze m6A modification as the writers. Demethylases fat mass and obesity-associated protein (FTO) and AlkB homolog 5 (ALKBH5) function as the erasers, removing methylation from substrates. Many m6A-binding proteins, including insulin-like growth factor 2 mRNA binding proteins (IGF2BP1/2/3), YTH domain-containing proteins (YTHDC1/2) and YTH family proteins (YTHDF1/2/3), function as the readers, recognizing and binding m6A-modified transcripts to mediate different biological effects (Lan et al. 2019).

m6A modifications have been implicated in inflammatory responses, including those observed during IBD (Luo et al. 2021). Further, m6A regulators are differentially expressed in IBD and are correlated with innate immune cell infiltration (Chen et al. 2021). Depletion of *Mettl3* in intestinal porcine epithelial cell line J2 decreased m6A level on *Traf6* transcripts, suppressing their nuclear export, which led to a decrease in Traf6 levels and subsequent inhibition of NF-κB and mitogen-activated protein kinases (MAPK) signalings, thus suppressing inflammation in response to lipopolysaccharide (LPS) treatment (Zong et al. 2019). In another study, knocking down METTL3 in mouse intestinal epithelial cells with LPS treatment resulted in enhanced cell viability, inhibition of apoptosis, and downregulation of pro-inflammatory cytokines, and phosphorylation of NF-κB p65, in addition to ameliorating dextran sulfate sodium (DSS)-induced IBD in mice (Yang et al. 2022). Silencing METTL14 inhibited the apoptosis of spinal cord neurons and alleviated spinal cord injury through inhibiting EEF1A2 m6A modification and activation of the Akt/mTOR signaling (Gao et al. 2022). Thus, the m6A modification plays different roles under various inflammatory conditions, which may be mediated via different mechanisms.

LncRNAs, transcripts > 200 nucleotides in length, modulate various biological and pathological processes (Lin et al. 2020). Serving as competing endogenous RNAs (ceRNAs), lncRNAs regulate miRNA functions through sponging miRNAs and regulating their expressions, whereas miRNAs promote target gene degradation through binding with the 3′-UTR of mRNAs (Entezari et al. 2022). LncRNAs can also be modified by m6A, which affects their stability and/or localization through interactions between lncRNAs, proteins, miRNAs, and mRNAs (He et al. 2020). The roles of lncRNA m6A modifications in tumorigenesis and other pathological processes are now a field of active research (Zheng et al. 2022; Wu et al. 2022). Li et al. observed differential m6A levels for 90 lncRNAs in pro-inflammatory M1-like versus anti-inflammatory M2-like primary rat microglia, which affected multiple pathways implicated in the inflammatory response (Li et al. 2021). METTL14 knockdown in colorectal cancer cells led to reduced m6A

levels on the lncRNA XIST, enhancing its expression and tumor-promoting effects (Yang et al. 2020). Another study examined doxorubicin-induced ferroptosis in myocardial injury and found that METTL14 catalyzed m6A modification of lncRNA KCNQ1OT1 to increase its stability in an IGF2BP1-dependent manner, whereafter KCNQ1OT1 sponged miR-7-5p to upregulate transferrin receptor levels, promoting iron uptake and lipid reactive oxygen species production in AC16 cardiomyocytes (Zhuang et al. 2023). m6A demethylase FTO promoted epithelial-to-mesenchymal transition process and inflammatory response by reducing the m6A modification of lncRNA GAS5 in transforming growth factor-β1-treated proximal tubular epithelial cells and a unilateral ureteral occlusion-constructed renal interstitial fibrosis mouse model (Li et al. 2022). Previously, we observed reduced METTL14 expression in UC and TNF-α-treated Caco-2 cells (Wu et al. 2024). However, whether METTL14 regulates the expression of lncRNAs through m6A modification in UC remains unexplored.

Here, we performed lncRNA sequencing and functional studies to examine the roles of METTL14 in lncRNA regulation in UC. We revealed that silencing METTL14 expression decreases the survival of Caco-2 cells stimulated by TNF-α, enhances inflammatory responses, and aggravates DSS-induced colitis in mice. Moreover, knocking down METTL14 exerts a pro-inflammatory effect via the DHRS4-AS1/miR-206/adenosine A3 receptor (A3AR) axis. Mechanistically, METTL14 modulates DHRSA-AS1 expression in m6A-dependent manners. The findings can facilitate understanding the relevance of m6A modifications during UC pathogenesis.

Materials and methods

Cell culture, treatment, and transfection

Caco-2 human colorectal carcinoma cells were acquired from the Cell Bank of Type Culture Collection of the Chinese Academy of Sciences (Shanghai, China. The cells were incubated in RPMI1640 medium (Yeasen, Shanghai, China) supplemented with 10% fetal bovine serum (Sigma-Aldrich, MO, USA) in a 37 °C incubator containing 5% CO_2. A cellular inflammation model was created in the cells via TNF-α (PeproTech, CA, USA) exposure. For 3-deazaadenosine (DAA) treatment, 50 μM DAA (APExBIO, Houston, USA) was added to complete media and 12-h incubated with cells. For JSH-23 (an NF-κB signaling inhibitor) treatment, Caco-2 cells were 3-h pretreated with 30 μM JSH-23, followed by TNF-α stimulation. For METTL14 knockdown, negative control small interfering RNAs (siRNAs) (si-NC) and siRNA against METTL14 (si-METTL14) were synthesized by Ribo bio (Guangzhou, China). Lentivirus containing small hairpin RNA (shRNA) targeting METTL14 (sh-METTL14) and the negative control (sh-NC) were acquired from GeneChem (Shanghai, China). The target sequence of METTL14 was 5′- GCATTGGTGCCGTGTTAAATA -3′. The stably transfected cells were selected by utilizing 2 μg/mL puromycin. For DHRS4-AS1 overexpression, the DHRS4-AS1 full-length sequence was cloned into pcDNA3.1 by Obio Company (Shanghai, China) to construct an overexpression plasmid (OE-DHRS4-AS1). The pcDNA3.1 empty vector (OE-NC) was used as a negative control. For miR-206 overexpression, the miR-206 mimic and corresponding negative control (mimic-NC) were acquired from Ribo bio. The siRNA, plasmid, or mimic was transfected into Caco-2 cells utilizing Lipofectamine 2000 (Thermo Fisher Scientific, CA, USA). Overexpression or knockdown efficiencies were assessed via RT-qPCR and western blotting.

Animal experiment

Eight-week male C57BL/6 mice (20–22 g in weight) were acquired from Yancheng Biotechnology Co., Ltd. (Guangzhou, China) and housed in a standard breeding setting for a one-week quarantine period. The experimental protocol adhered to the Guide for the Care and Use of Laboratory Animals issued by the US National Research Council and received the approvement from the Animal Ethics and Welfare Committee of the Affiliated Hospital of Guangdong Medical University. Colitis was induced by adding 3% DSS (MP Biomedicals, CA, USA) into the drinking water for seven days. The control group received distilled water. Twenty-four mice were randomly separated (n = 6 per group) into four groups: (1) control, (2) DSS, (3) DSS + Ad-sh-NC (a negative control adenovirus vector, Obio), and DSS + Ad-sh-METTL14 (an adenovirus containing METTL14

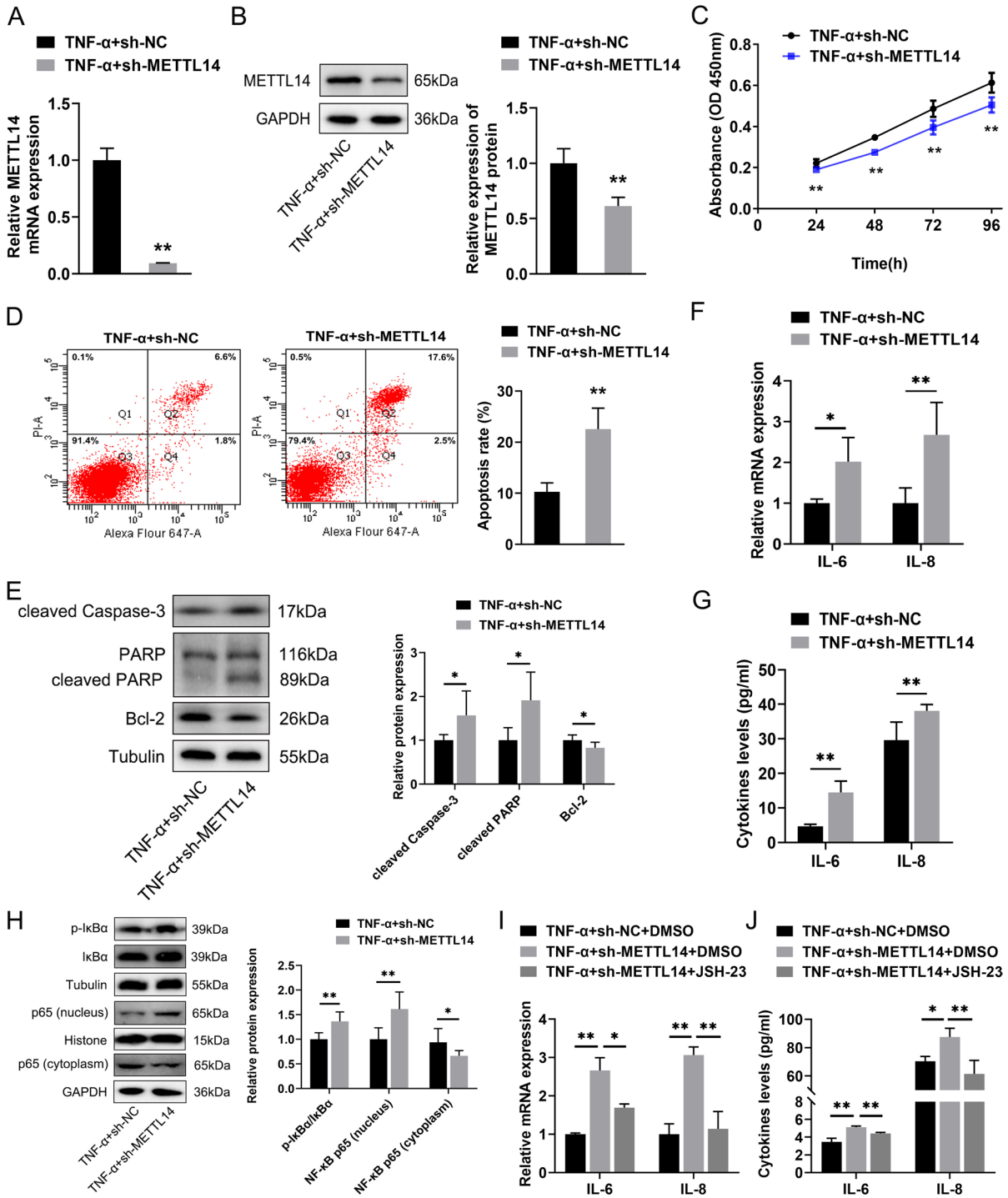

short hairpin RNA, Obio). Ad-sh-NC or Ad-sh-METTL14 (10^9 PFUs per mouse) was injected into mice via the tail vein on days 1 and 4 during DSS administration.

The daily assessment of mice included monitoring their body weight, the blood presence in stool, and stool consistency, for calculating the disease activity index (DAI) according to a previously established

◂**Fig. 1** METTL14 knockdown promoted TNF-α-induced Caco-2 cell inflammatory injury. Caco-2 cells were transfected with sh-NC or sh-METTL14 lentivirus, and treated with TNF-α. **A** and **B** METTL14 expression was detected using RT-qPCR and western blotting. **C** Cell viability was analyzed using CCK-8 assays. **D** Apoptosis was detected via flow cytometry. **E** The expression levels of cleaved Caspase-3, cleaved PARP, and Bcl-2 were detected via western blotting. **F** The mRNA expression levels of IL-6 and IL-8 were assessed via RT-qPCR. **G** The concentrations of IL-6 and IL-8 were detected via ELISA. **H** The expressions of p-IκBα, and NF-κB levels in both nucleus and cytoplasm were measured via western blotting. Caco-2 cells were divided into sh-NC + DMSO, sh-METTL14 + DMSO, and sh-METTL14 + JSH-23 groups, and all groups were stimulated with TNF-α. **I** The mRNA expression levels of IL-6 and IL-8 were assessed via RT-qPCR. **J** The concentrations of IL-6 and IL-8 were detected via ELISA. The data are presented as mean ± SD. All data were obtained from at least three replicate experiments. $^{*}P < 0.05$ and $^{**}P < 0.01$

method (Ding et al. 2018). The mice were sacrificed by isoflurane anesthesia and cervical dislocation. Colon samples were collected on day 8 for further analysis. Colon length was recorded, and the colon tissues were saved in liquid nitrogen for subsequent use. For histological analysis, the colon tissues were immersed in 4% paraformaldehyde followed by paraffin embedding. These tissues were then sliced and received hematoxylin and eosin (H&E) staining for observation utilizing a microscope.

RT-qPCR analysis

Total RNA was isolated from the cells utilizing AG RNAex Pro Reagent (AGbio, Hunan, China). For mRNA and lncRNA analyses, RNA was converted into cDNA using HiScript III RT kit (Vazyme, Nanjing, China). For miRNA analysis, the miRNA was reversely transcribed utilizing the Mir-X miRNA First-Strand Synthesis Kit (Clontech Laboratories, USA). qPCR was conducted on a LightCycler® 480 II system (Roche AG, Basel, Switzerland). MiRNA expression was normalized against U6 small nuclear RNA. mRNA and lncRNA expressions were normalized against β-actin. The sequences of the primers utilized were summarized in Supplementary Table S1.

LncRNA sequencing

Total RNA was extracted from si-METTL14- or si-NC-transfected Caco-2 cells with TNF-α treatment and analyzed via lncRNA sequencing (LC-BIO, Hangzhou, China) with Illumina NovaSeq 6000. The significant differentially expressed lncRNAs were selected based on log2 (fold change) > = 1 or < = − 1 and P value < 0.05.

Western blotting

Protein extraction was performed on Caco-2 cells and mouse colon tissues utilizing the RIPA lysis buffer (Beyotime, Shanghai, China), with phosphatase inhibitors cocktail and phenylmethylsulfonyl fluoride (Beyotime) supplementation. The nuclear and cytoplasmic proteins were extracted utilizing a nuclear and cytoplasmic extraction kit (CWBio, Jiangsu, China). Subsequently, the proteins were separated via SDS-PAGE and transferred onto polyvinylidene difluoride membranes (Millipore, MA, USA). After 5% non-fat milk blocking, primary antibodies (Supplementary Table S2) were added for membranes incubation. Then the secondary antibodies (Beyotime) were added for 1-h membranes incubation. The protein bands were detected using an ECL chemiluminescent substrate detection kit (hypersensitive) (APExBIO).

Analysis of inflammatory cytokines and myeloperoxidase (MPO) activity

The IL-6 and IL-8 levels in the culture medium supernatant of Caco-2 cells after different treatment as well as the TNF-α and IL-6 levels in mouse colon tissues were measured utilizing corresponding enzyme-linked immunosorbent assay (ELISA) kits (Neobioscience, Shenzhen, China; Meimian, Jiangsu, China). The 450-nm optical density was measured with a microplate reader. MPO activity in mouse colon tissues was assessed using an MPO activity kit (Jiancheng, Nanjing, China).

Cell viability assay

After the experimental treatment, the cells in each well were added with the cell counting kit-8 (CCK-8) reagent (APExBIO) at indicated time points. Cell viability was assessed at the 450-nm optical density utilizing a microplate reader.

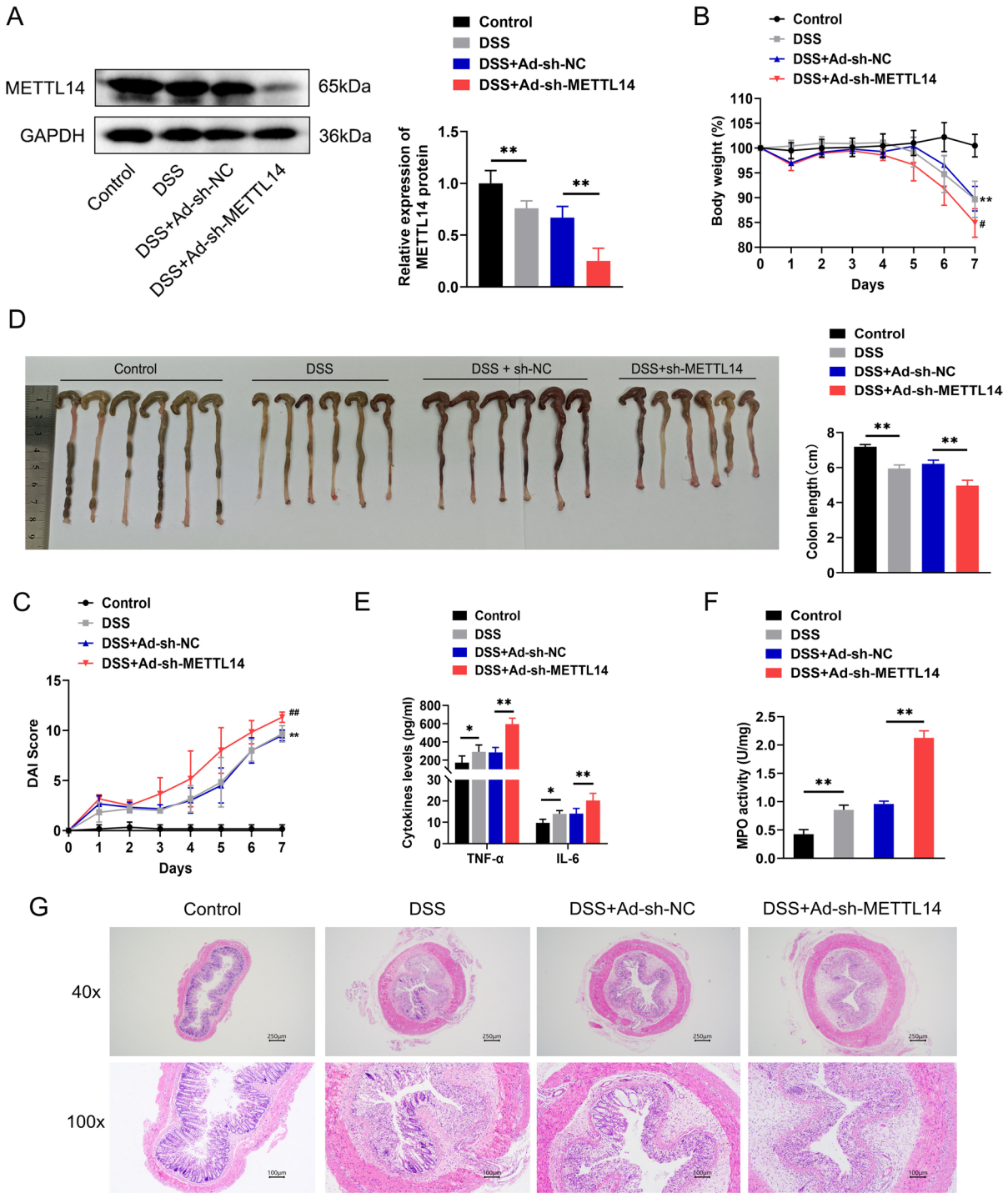

Fig. 2 METTL14 knockdown promoted colitis development in mice. Colitis was induced by DSS, and Ad-sh-NC or Ad-sh-METTL14 was injected to mice via the tail vein. **A** METTL14 expression in the colon tissues of mice was detected via western blotting. **B** Changes of body weight. **C** The DAI scores. **D** The colon lengths. **E** TNF-α and IL-6 levels in the colon tissues were detected via ELISA. **F** MPO activity in the colon tissues. **G** Representative histopathologic image of colon stained with H&E. The data are presented as mean ± SD. n = 6 per group. ** $P < 0.01$ compared with Control group; # $P < 0.05$, ## $P < 0.01$ compared with the DSS + Ad-sh-NC group in panels **B** and **C**. * $P < 0.05$ and ** $P < 0.01$ in other panels

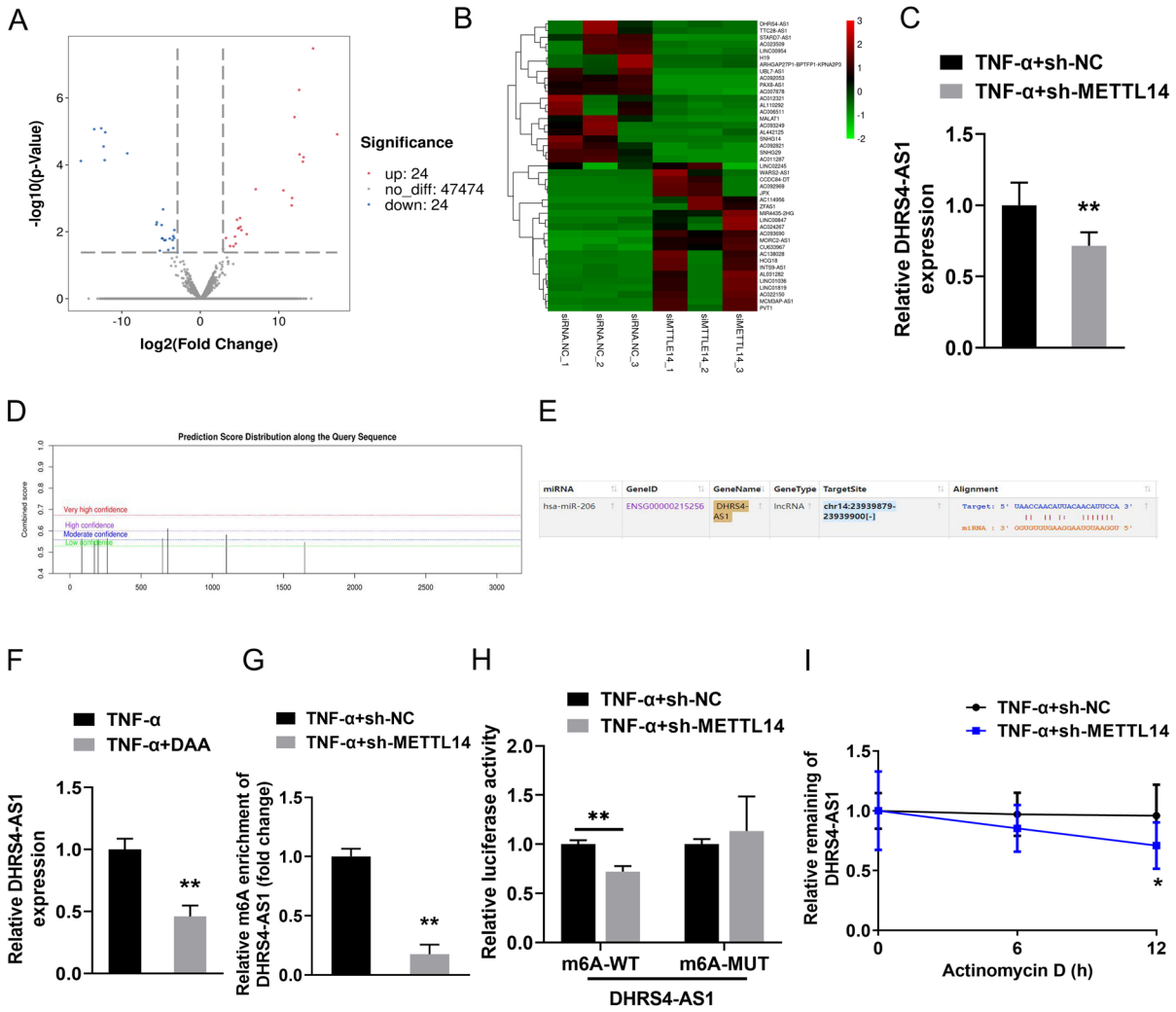

Fig. 3 METTL14 knockdown downregulated DHRS4-AS1 through lower m6A modification. **A** LncRNA sequencing was used to analyze differentially expressed lncRNAs between TNF-α-treated Caco-2 cells subjected to si-METTL14 or si-NC transfection. Differentially expressed lncRNAs are shown in the volcano plot. **B** Differentially expressed lncRNAs are shown in the heat map. **C** DHRS4-AS1 expression was detected via RT-qPCR in Caco-2 cells subjected to METTL14 knockdown and TNF-α treatment. **D** The m6A modification sites within DHRS4-AS1 sequence were predicted using SRAMP database (http://www.cuilab.cn/sramp). **E** The binding site for miR-206 within the DHRS4-AS1 sequence was predicted using the StarBase database (http://starbase.sysu.edu.cn/mirMrna.php). **F** The expression of DHRS4-AS1 was detected via RT-qPCR following TNF-α and DAA treatment. **G** The m6A level of DHRS4-AS1 was examined via MeRIP-qPCR in Caco-2 cells with METTL14 knockdown and TNF-α treatment. **H** Relative luciferase activity in sh-METTL14 or sh-NC cells transfected with DHRS4-AS1-m6A-WT or MUT reporter plasmid**. I** RNA stability analysis was performed in Caco-2 cells with METTL14 knockdown after treatment with actinomycin D. The data are presented as mean ± SD. All data were obtained from at least three replicate experiments. *$P < 0.05$ and **$P < 0.01$

Apoptosis assay

The cells were resuspended in the binding buffer and subsequently labeled with the Annexin V-Alexa Fluor647 and PI (Yeasen) for a duration of 15 min. Then the cells were analyzed via flow cytometry (BD, NJ, USA).

Dual-luciferase reporter assay

The SRAMP (http://www.cuilab.cn/sramp) online tool was used to predict the potential m6A sites in the DHRS4-AS1 sequence. Adenosine (A) bases within the "RRACH motif" were replaced with thymine

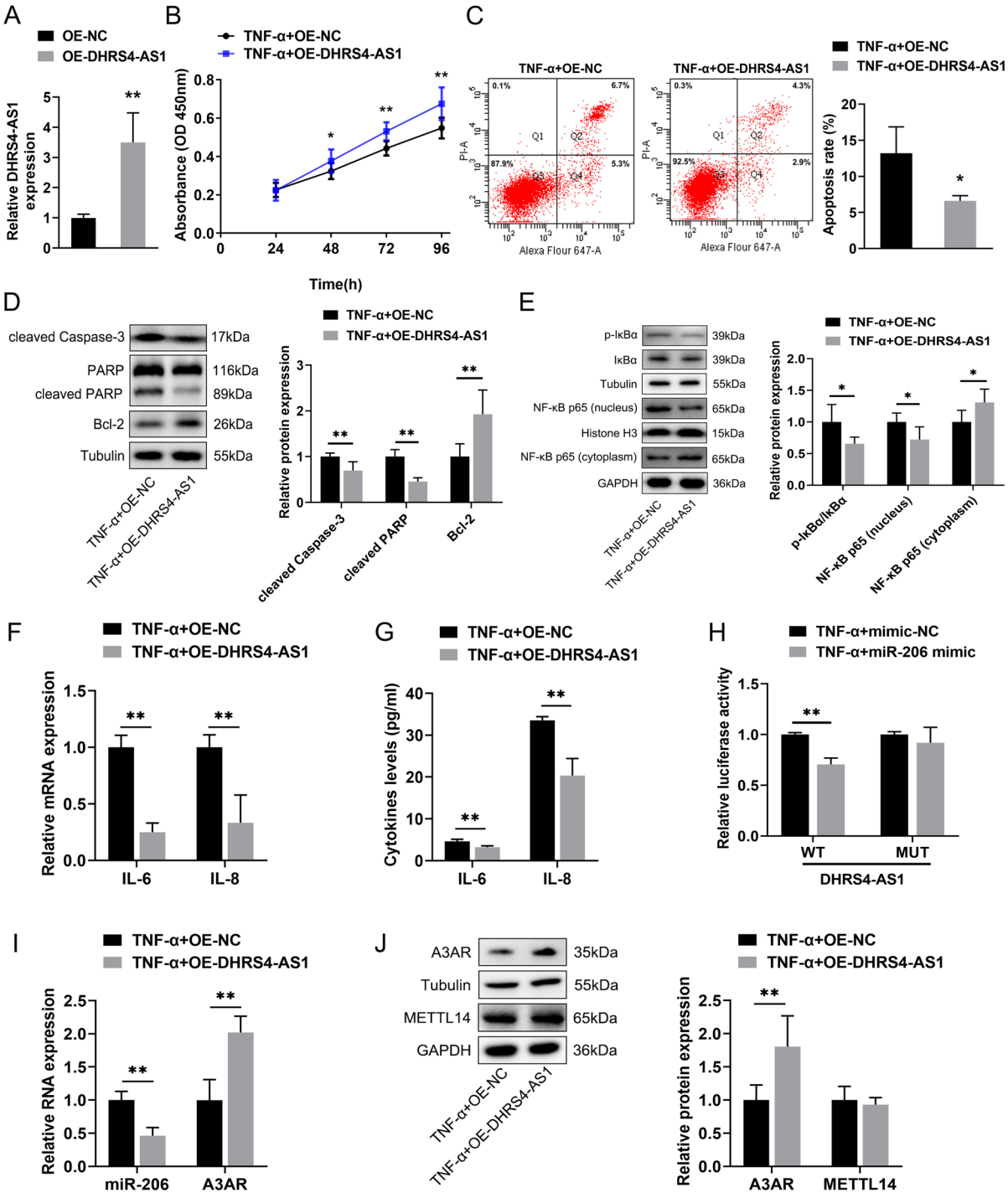

(T) and inserted into GV306 vectors to construct the mutant reporter plasmid. The mutant (DHRS4-AS1-m6A-MUT) and wild-type (DHRS4-AS1-m6A-WT) dual-luciferase reporter plasmids were synthesized by GeneChem. The potential miR-206 binding site in DHRS4-AS1 was predicted utilizing StarBase (http://starbase.sysu.edu.cn/mirMrna.php) and mutated in the DHRS4-AS1 sequence. The mutant (MUT) or

◂**Fig. 4** LncRNA DHRS4-AS1 inhibited inflammatory injury in TNF-α-stimulated Caco-2 cells. Caco-2 cells were transfected with an OE-NC or OE-DHRS4-AS1 plasmid, and treated with TNF-α. **A** DHRS4-AS1 expression was detected using RT-qPCR. **B** Cell viability was analyzed using CCK-8 assays. **C** Apoptosis was detected via flow cytometry. **D** The levels of cleaved Caspase-3, cleaved PARP, and Bcl-2 were detected via western blotting. **E** The expression of p-IκBα, and NF-κB levels in both nucleus and cytoplasm were measured via western blotting. **F** The mRNA expression levels of IL-6 and IL-8 were assessed via RT-qPCR. **G** The concentrations of IL-6 and IL-8 were detected via ELISA. **H** Relative luciferase activities in Caco-2 cells co-transfected with DHRS4-AS1-WT or MUT reporter plasmid and miR-206 mimic or mimic-NC**. I** The expression of miR-206 and A3AR mRNA was measured via RT-qPCR. **J** The levels of A3AR and METTL14 protein were detected via western blotting. The data are presented as mean ± SD. All data were obtained from at least three replicate experiments. *$P < 0.05$ and **$P < 0.01$

wild-type (WT) DHRS4-AS1 sequence containing a putative miR-206 binding site was cloned into the GV306 vectors, named as DHRS4-AS1-MUT or DHRS4-AS1-WT, respectively, which were synthesized by GeneChem. For the dual-luciferase reporter assay, sh-NC and sh-METTL14 cells were transfected with DHRS4-AS1-m6A-MUT or DHRS4-AS1-m6A-WT. Alternatively, Caco-2 cells were co-transfected with the mimic-NC or miR-206 mimic and DHRS4-AS1-MUT or DHRS4-AS1-WT. Transfections were carried out using Lipofectamine 2000. Luciferase activities were quantified utilizing a Dual Luciferase Reporter Assay Kit (Yeasen), with the relative activities expressed as in ratios of the firefly and Renilla luciferase activities.

RNA stability analysis

The cells received 24-h TNF-α treatment followed by 7.5 μg/mL actinomycin D (Sigma-Aldrich) treatment for 0, 6, and 12 h. DHRS4-AS1 expression was assessed using RT-qPCR.

Methylated RNA immunoprecipitation (MeRIP)-qPCR

The EpiQuik™ m6A RNA Enrichment (MeRIP) Kit (Epigentek, NY, USA) was utilized for MeRIP analyses. Total RNA was isolated, and then was immunoprecipitated using an m6A antibody or IgG antibody linked to affinity beads in immune capture buffer for 90 min at room temperature. RNA was eluted and purified. DHRS4-AS1 levels were analyzed via RT-qPCR. The enrichment level of m6A was standardized relative to the input.

Statistical analysis

All experimental data are from at least triplicates, and are expressed in mean ± SD. All statistical analyses were conducted utilizing SPSS 19.0 (IBM Corp. NY, Armonk, USA). Two-tailed Student's *t*-tests were carried out to assess between-group differences. One-way ANOVAs followed by Tukey's post-hoc analyses were employed for comparisons involving multiple groups. Statistical significance was defined as $P < 0.05$.

Results

METTL14 knockdown promoted Caco-2 cell inflammatory injury

To investigate the biological function of METTL14 during inflammatory injury, a lentivirus-mediated shRNA approach was employed to silence METTL14 in Caco-2 cells (Fig. 1A, B). Subsequently, the impact of METTL14 knockdown was examined on cell viability, apoptosis, and inflammatory response following TNF-α treatment. METTL14 silencing resulted in notably decreased viability of Caco-2 cells and a significant elevation in the apoptosis rate, in comparison to the sh-NC group (Fig. 1C, D). In addition, cleaved PARP and cleaved Caspase-3 proteins were markedly upregulated, while Bcl-2 was downregulated following METTL14 silencing (Fig. 1E). Furthermore, METTL14 knockdown significantly elevated the IL-6 and IL-8 expressions in Caco-2 cells (Fig. 1F, G). NF-κB signaling was also enhanced, as reflected by the nuclear NF-κB p65 and p-IκBα upregulation (Fig. 1H). The inflammatory effects triggered by METTL14 knockdown were partially attenuated by treatment with JSH-23, an inhibitor of NF-κB (Fig. 1I, J). Collectively, these data suggest that the knockdown of METTL14 exacerbates TNF-α-induced inflammation in Caco-2 cells through activation of the NF-κB pathway.

METTL14 knockdown promoted colitis development in mice

The effect of METTL14 knockdown on DSS-induced colitis was investigated in mice. We silenced

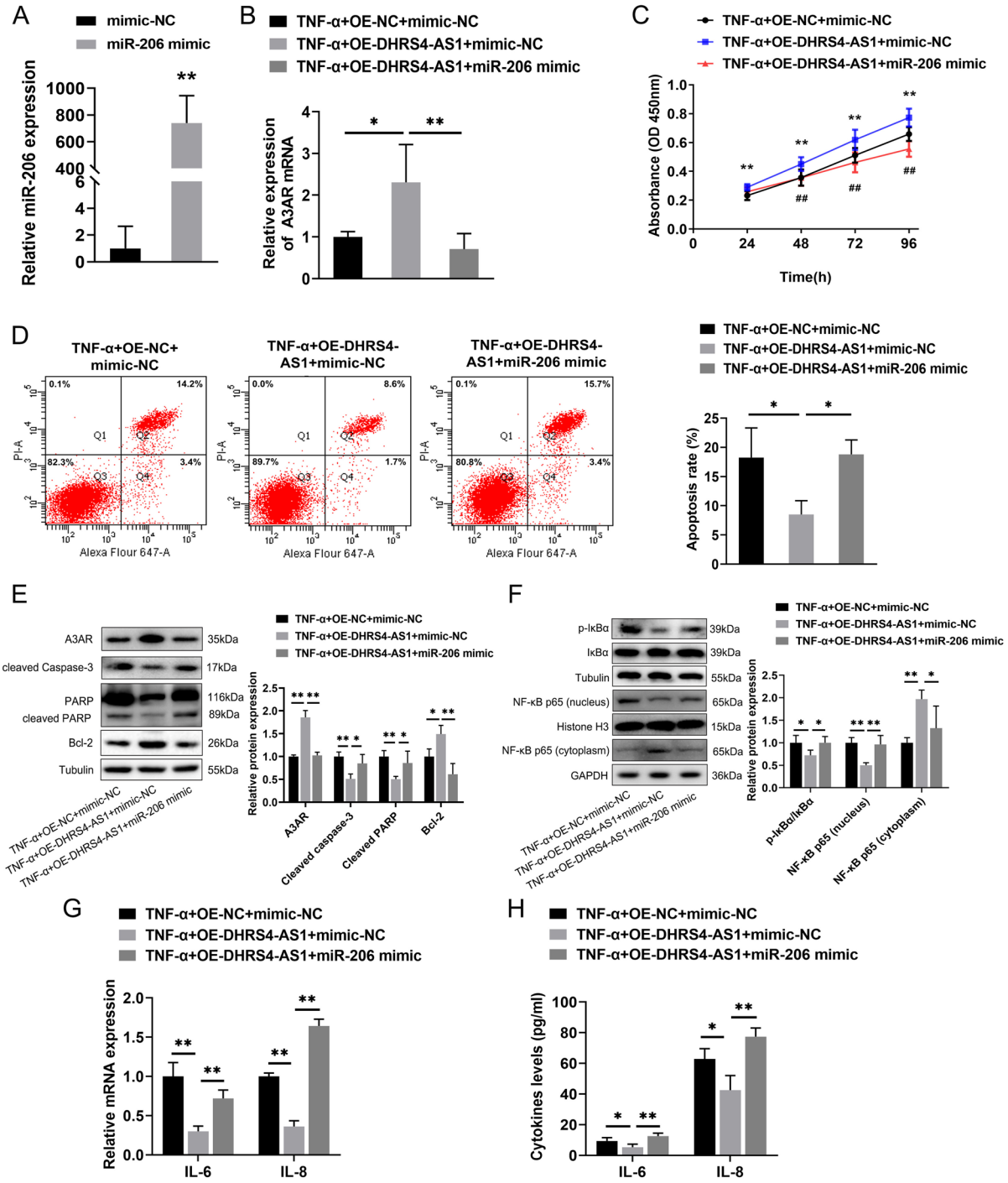

METTL14 expression in DSS-treated mice by injecting Ad-sh-NC (control) or Ad-sh-METTL14 via the tail vein. METTL14 expression was decreased by DSS treatment and further suppressed by Ad-sh-METTL14 in the colon tissues of mice (Fig. 2A). Following DSS treatment, mice displayed significant weight loss, an elevated DAI, and a reduced colon length compared to those of control group mice. METTL14 knockdown exacerbated these effects, resulting in a more severe weight reduction

◂**Fig. 5** miR-206 mediated the effect of DHRS4-AS1 on inflammatory injury of TNF-α-stimulated Caco-2 cells. **A** miR-206 expression in Caco-2 cells following mimic-NC or miR-206 mimic transfection was detected using RT-qPCR. Caco-2 cells were divided into OE-NC + mimic-NC, OE-DHRS4-AS1 + mimic-NC, and OE-DHRS4-AS1 + miR-206 mimic groups, and all groups were stimulated with TNF-α. **B** The expression of A3AR mRNA was assessed via RT-qPCR. **C** Cell viability was analyzed using CCK-8 assays. **D** Apoptosis was detected via flow cytometry. **E** The levels of A3AR, cleaved Caspase-3, cleaved PARP, and Bcl-2 were detected via western blotting. **F** The expression of p-IκBα and NF-κB levels in both nucleus and cytoplasm were detected via western blotting. **G** The mRNA expressions of IL-6 and IL-8 were assessed via RT-qPCR. **H** The concentrations of IL-6 and IL-8 were detected via ELISA. The data are presented as mean ± SD. All data were obtained from at least three replicate experiments. ** $P < 0.01$ compared with TNF-α + OE-NC + mimic-NC group; ## $P < 0.01$ compared with TNF-α + OE-DHRS4-AS1 + mimic-NC group in panel **C**.*$P < 0.05$ and **$P < 0.01$ in other panels.

and a further increased DAI (Fig. 2B, C). In addition, METTL14 knockdown promoted DSS-induced colon shortening in mice (Fig. 2D). Furthermore, the IL-6 and TNF-α levels and the MPO activity were elevated in colitis tissues compared to those in control tissues. METTL14 silencing significantly upregulated cytokine expression and MPO activity (Fig. 2E, F). H&E staining of colon tissue revealed that DSS caused the destruction of the colonic mucosa, abnormal crypt structure, and inflammatory cell infiltration. METTL14 knockdown worsened these histopathological changes, as reflected by extensive colonic mucosal injury, loss of crypt structure, and greater inflammatory cells infiltration (Fig. 2G). The findings demonstrate that METTL14 knockdown aggravates colonic inflammation in mice treated with DSS.

METTL14 knockdown downregulated DHRS4-AS1 through lower m6A modification

To uncover lncRNA expression changes resulting from METTL14 knockdown, lncRNA sequencing was performed in si-METTL14- and si-NC-transfected Caco-2 cells following TNF-α treatment. The results revealed a significant dysregulation of 48 lncRNAs following METTL14 knockdown. Among these potential targets, we identified lncRNA DHRS4-AS1 and validated its altered expression using RT-qPCR (Fig. 3A-C). Using the SRAMP database, we predicted potential m6A sites within the DHRS4-AS1 sequence (Fig. 3D). We also identified a potential binding site for miR-206 within the DHRS4-AS1 sequence using the StarBase database (Fig. 3E). In our previous studies, we observed that activation of A3AR, a target of miR-206, was anti-inflammatory through suppressing the NF-κB signaling pathway in TNF-α-stimulated human colonic epithelial cells (Ren et al. 2014). Further, miR-206 was found to promote inflammatory responses in UC by decreasing the expression of A3AR and activating the NF-κB signaling (Wu et al. 2017). Given these findings, we hypothesized that METTL14 might regulate colonic inflammation through the lncRNA DHRS4-AS1/miR-206/A3AR axis. Consequently, we focused on DHRS4-AS1 in our following experiments. To examine the roles of m6A modification in regulating DHRS4-AS1, we treated Caco-2 cells with DAA, a global methylation inhibitor. Notably, significantly reduced DHRS4-AS1 expression was observed in the TNF-α + DAA-treated group relative to that in the TNF-α-treated group (Fig. 3F). Furthermore, MeRIP-qPCR revealed that the m6A level of DHRS4-AS1 was substantially reduced following knocking down METTL14 in the Caco-2 cells (Fig. 3G). Additionally, we mutated DHRS4-AS1 m6A sites (5′-RRACU-3′ to 5′-RRTCU-3′) to construct luciferase reporters containing either the WT or MUT motifs to explore the effect of METTL14-mediated m6A modification on DHRS4-AS1 expression. METTL14 silencing resulted in the decrease of luciferase activity in the wide-type DHRS4-AS1 reporter but had no effect on the mutated one (Fig. 3H). Furthermore, treating with actinomycin D revealed that knocking down METTL14 significantly accelerated the decay of DHRS4-AS1 in the Caco-2 cells with TNF-α treatment (Fig. 3I). To summarize, these data suggested that DHRS4-AS1 was a target of METTL14-mediated m6A modification.

LncRNA DHRS4-AS1 inhibited the inflammatory injury in Caco-2 cells via the miR-206/A3AR *axis*

To further assess the biological role of DHRS4-AS1, we transfected Caco-2 cells with a DHRS4-AS1 overexpression plasmid (OE-DHRS4-AS1) (Fig. 4A). When DHRS4-AS1 was overexpressed, the viability of TNF-α-treated Caco-2 cells was significantly elevated, whereas their rate of apoptosis was reduced (Fig. 4B, C). Furthermore, DHRS4-AS1

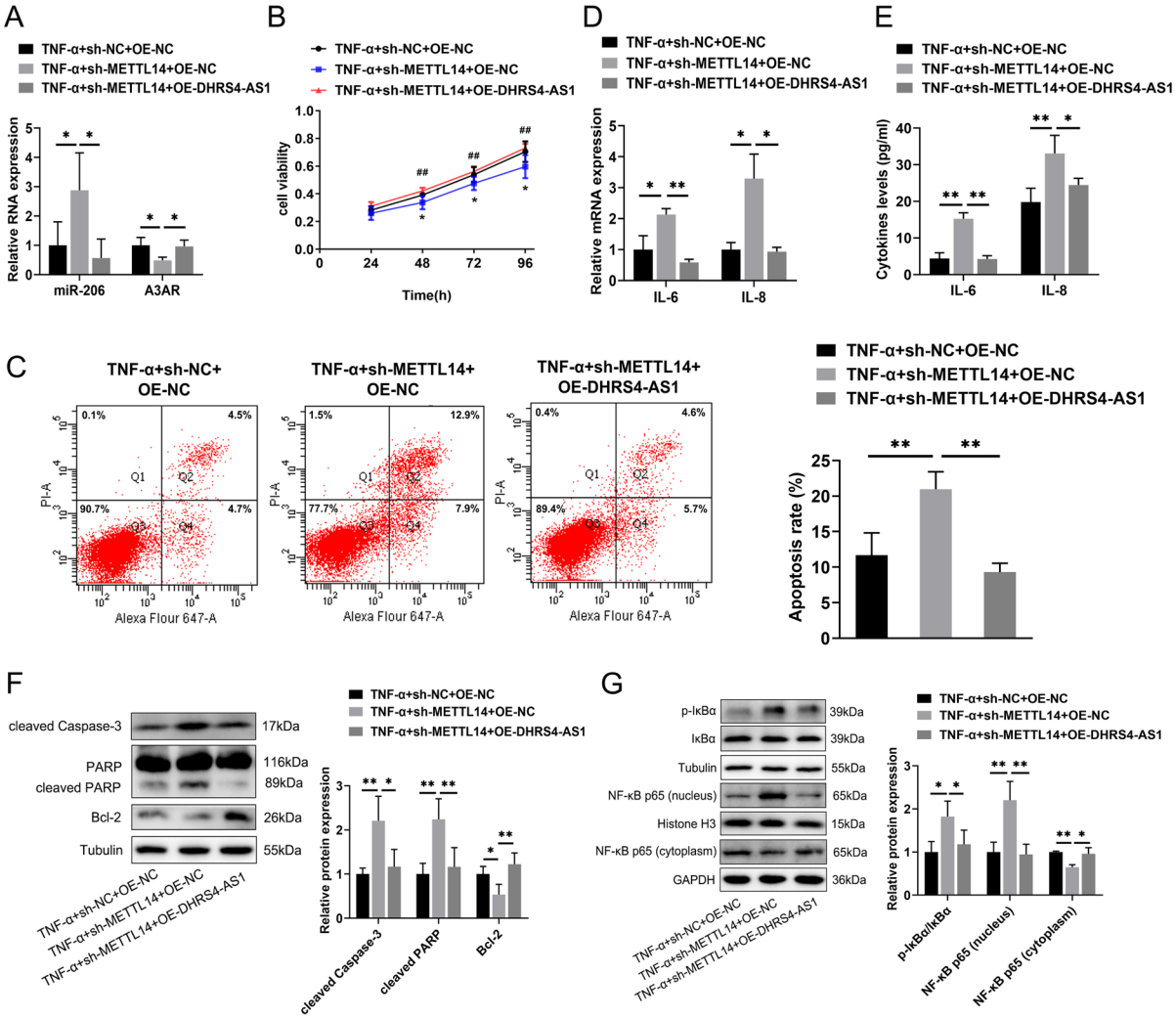

Fig. 6 The pro-inflammatory functions of METTL14 silencing were mediated via DHRS4-AS1. Caco-2 cells were divided into sh-NC + OE-NC, sh-METTL14 + OE-NC, and sh-METTL14 + OE-DHRS4-AS1 groups, and all groups were stimulated with TNF-α. **A** The expression levels of miR-206 and *A3AR* mRNA were assessed via RT-qPCR. **B** Cell viability was analyzed using CCK-8 assays. **C** Apoptosis was detected via flow cytometry. **D** The mRNA expression levels of IL-6 and IL-8 were assessed via RT-qPCR. **E** The concentrations of IL-6 and IL-8 were detected via ELISA. **F** The levels of cleaved Caspase-3, cleaved PARP, and Bcl-2 were detected via western blotting. **G** The expression of p-IκBα and NF-κB levels in both nucleus and cytoplasm were determined via western blotting. The data are presented as mean ± SD. All data were obtained from at least three replicate experiments. * $P < 0.05$ compared with TNF-α + sh-NC + OE-NC group; ## $P < 0.01$ compared with TNF-α + sh-METTL14 + OE-NC group in panel **B**.*$P < 0.05$ and **$P < 0.01$ in other panels

overexpression led to remarkable downregulation of cleaved Caspase-3 and cleaved PARP proteins as well as an upregulation of Bcl-2 (Fig. 4D). The expressions of nuclear NF-κB p65 and p-IκBα and the levels of IL-6 and IL-8 were significantly inhibited (Fig. 4E-G). Taken together, our data suggest that DHRS4-AS1 attenuated the inflammatory injury in Caco-2 cells caused by TNF-α. As bioinformatics analysis revealed a potential binding site for miR-206 in DHRS4-AS1, we hypothesized that the effect of DHRS4-AS1 is mediated via miR-206. Dual-luciferase reporter assays were carried out to validate the interaction between DHRS4-AS1 and miR-206. The findings indicated that the miR-206 mimic remarkably suppressed luciferase activities in the DHRS4-AS1 WT group rather than those in the MUT group

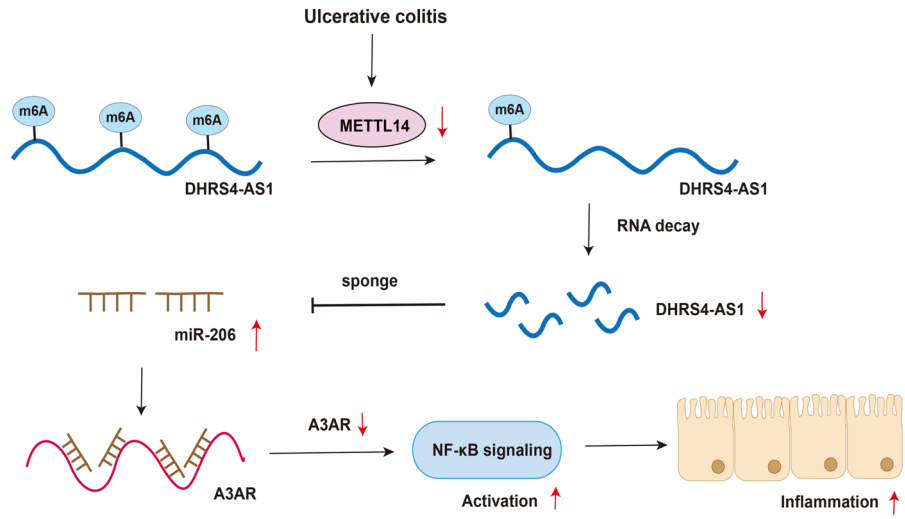

Fig. 7 A scheme of the proposed mechanisms: knockdown of METTL14 aggravated colonic inflammatory injury in UC by regulating the DHRS4-AS1/miR-206/A3AR axis through m6A modification of DHRS4-AS1

(Fig. 4H). Moreover, RT-qPCR and western blotting showed that overexpression of DHRS4-AS1 in Caco-2 cells reduced the level of miR-206 and increased A3AR expression, with no impact on METTL14 levels (Fig. 4I, J).

To confirm that DHRS4-AS1 exerted its anti-inflammatory effects via miR-206, we conducted rescue experiments via transfection of an miR-206 mimic in DHRS4-AS1-overexpressing Caco-2 cells under TNF-α stimulation (Fig. 5A). The enhanced A3AR expression induced by DHRS4-AS1 overexpression was partially abrogated by the miR-206 mimic (Fig. 5B and E). As indicated in Fig. 5C and D, the miR-206 mimic abolished the effects of DHRS4-AS1 overexpression on cell viability and reversed the reduced apoptosis rate in Caco-2 cells with TNF-α treatment. The downregulation of cleaved Caspase-3 and cleaved PARP proteins and upregulation of Bcl-2 under DHRS4-AS1 overexpression were partially counteracted by the miR-206 mimic (Fig. 5E). Further, the mimic nullified the inhibitory effect of DHRS4-AS1 overexpression on NF-κB signaling activation as well as IL-6 and IL-8 secretion (Fig. 5F-H). Collectively, the above results indicated that DHRS4-AS1 suppressed TNF-α-induced inflammatory injury by targeting the miR-206/A3AR axis.

METTL14 silencing's pro-inflammatory functions were mediated via *DHRS4-AS1*

To examine DHRS4-AS1's contribution in mediating the effect of METTL14, we overexpressed DHRS4-AS1 in METTL14-silenced Caco-2 cells. RT-qPCR analysis showed that DHRS4-AS1 reversed METTL14 knockdown-induced miR-206 upregulation and A3AR downregulation (Fig. 6A). DHRS4-AS1 overexpression partially suppressed the promoting effect of METTL14 knockdown on TNF-α-induced cell apoptosis and inflammation, while restoring the viability of Caco-2 cells (Fig. 6B-E). Western blotting further demonstrated that the overexpression of DHRS4-AS1 in METTL14-knockdown Caco-2 cells suppressed the cleaved PARP and cleaved Caspase-3 expressions as well as the p-IκBα and nuclear NF-κB levels (Fig. 6F, G). Overall, these findings suggest that the effects of METTL14 knockdown on TNF-α-induced cellular inflammatory injury were partially alleviated by DHRS4-AS1 overexpression.

Discussion

IBD is a chronic inflammatory disease with a characteristic remission-relapse pattern particularly prevalent in Westernized nations and with a rapidly growing incidence in more recently industrialized countries (Zeng et al. 2023). The severity and frequency of IBD flare-ups vary significantly among patients, with unpredictable relapses contributing to a reduced quality of life (Zeng et al. 2023). Hence, understanding the pathogenesis of UC is of utmost significance for effective management of this disease. M6A modification, which regulates the expression

and function of mRNAs and ncRNAs, has attracted considerable interest in inflammatory disease research (Su et al. 2023). Here, we demonstrated that silencing METTL14 reduces the viability of TNF-α-stimulated Caco-2 cells, promoting inflammation and exacerbating DSS-induced colitis in mice. In addition, METTL14 knockdown exerts a pro-inflammatory effect by modulating the DHRS4-AS1/miR-206/A3AR axis. Notably, we found that METTL14 regulates DHRSA-AS1 expression in an m6A-dependent manner. These results offer fresh perspectives on the molecular mechanisms of METTL14 in UC.

METTL14 serves as a pivotal component of methyltransferase complexes where it influences the catalytic activity of METTL3 and the specific recognition of RNA sequences (Zhou et al. 2021a). METTL14 has been extensively implicated in inflammation-related pathologies. A study revealed that METTL14 knockout in podocytes led to improvements in glomerular functions and mitigated podocyte injuries; these were featured by suppressing inflammation and apoptosis as well as activating autophagy in mice with adriamycin-induced nephropathy, through the m6A-dependent regulating of Sirt1 (Lu et al. 2021). Lu et al. (Lu et al. 2020) observed that spontaneous colitis could be triggered by T-cell METTL14 deficiency in mice, marked by a heightened infiltration of inflammatory cells, elevated levels of Th1 and Th17 cytokines, and dysfunctional Tregs. The complexity of METTL14 function across various inflammatory diseases may be attributed to distinct underlying mechanisms. We previously found the downregulation of METTL14 in UC tissues and TNF-α-treated Caco-2 cells (Wu et al. 2024). Herein, we demonstrated that knockdown of METTL14 exacerbated inflammatory injury in Caco-2 cells, as shown by decreased cell viability, greater apoptosis, higher levels of cleaved Caspase-3 and PARP, as well as reduced expression of Bcl-2. METTL14 knockdown led to a significant increase in NF-κB pathway activation and inflammatory cytokine production in Caco-2 cells with TNF-α treatment. In our murine model of colitis induced by DSS, METTL14 knockdown aggravated colonic damage and inflammation, as reflected by significant weight loss, elevated DAI scores, and increased TNF-α, IL-6 and MPO levels. These observations suggested that METTL14 protects against colonic inflammation.

Using lncRNA sequencing and RT-qPCR, we found that lncRNA DHRS4-AS1 was markedly downregulated after METTL14 knockdown. Bioinformatics analysis using the SRAMP m6A site predictor showed the existence of m6A sites within the DHRS4-AS1 transcript. This discovery led us to hypothesize that DHRS4-AS1 is a downstream target of METTL14. To validate this, we employed the universal methylation inhibitor DAA to demethylate RNA. Our results showed that DHRS4-AS1 expression significantly decreased following treatment with DAA. Moreover, MeRIP-qPCR confirmed a remarkable reduction in the levels of m6A-modified DHRS4-AS1 after METTL14 knockdown. Luciferase reporter assays further validated that METTL14-mediated m6A modification influenced DHRS4-AS1 expression. Actinomycin D treatment also indicated that METTL14 knockdown reduced DHRS4-AS1 stability. Collectively, these results demonstrated that DHRS4-AS1 stability is regulated by METTL14-mediated m6A modification. DHRS4-AS1 overexpression partially reversed the promotive effects of knocking down METTL14 on inflammatory injury in Caco-2 cells treated with TNF-α. These findings suggest that METTL14 performs its role by regulating DHRS4-AS1.

In hepatocellular carcinoma, non-small cell lung cancer, and gastric cancer, the lncRNA DHRS4-AS1 functions as a tumor suppressor (Zhou et al. 2021b; Yan et al. 2020; Xiao et al. 2023). Cui et al. demonstrated that in endometriosis, DHRS4-AS1 suppresses the ectopic endometrial stromal cells' invasion, migration, and proliferation while promoting apoptosis (Cui et al. 2022). Through gain-of-function experiments, we discovered that DHRS4-AS1 has an anti-inflammatory function during colonic cell inflammation, as indicated by the enhanced viability of Caco-2 cells, reduced apoptosis rates, as well as the suppressed NF-κB pathway activation and inflammatory cytokine production. StarBase predicted a binding interaction between miR-206 and DHRS4-AS1. We earlier found that miR-206 promotes inflammation in UC by decreasing the expression of its target gene A3AR and activating NF-κB signaling pathway (Wu et al. 2017). Therefore, we hypothesized that DHRS4-AS1 might exert its effects via binding to miR-206. In line with this notion, we found that DHRS4-AS1 negatively regulated miR-206 expression, with an miR-206 mimic effectively reversing the enhanced A3AR expression and anti-inflammatory effects of DHRS4-AS1 overexpression in Caco-2 cells with TNF-α treatment. The luciferase

reporter assay results validated the interaction between DHRS4-AS1 and miR-206. Taken together, these data suggested that DHRS4-AS1 mitigates inflammatory injury by targeting the miR-206/A3AR axis. However, our study has some limitations. First, we did not conduct MeRIP-seq, which may result in some omissions of important downstream lncRNAs. Second, we did not investigate the m6A-binding proteins worked with METTL14 in m6A-modified DHRS4-AS1. Future work should address these issues as well as identify other transcripts and mechanisms regulated by m6A modification in UC.

In conclusion, our work demonstrates that the knockdown of METTL14 aggravates colonic inflammatory injury in UC by regulating the DHRS4-AS1/miR-206/A3AR axis through m6A modification of DHRS4-AS1(Fig. 7). Our findings uncover a critical function of m6A-lncRNA and provide new insights into the pathogenesis of UC, highlighting METTL14 as a promising therapeutic target in this context.

Acknowledgements This work was funded by the Guangdong Province's Natural Science Foundation of Basic and Applied Basic Research (2024A1515013013), Competitive Allocation Project of Zhanjiang Municipal Science and Technology Development Special Fund (2021A05055, 2022A01165), and the High-level Talent Initial Scientific Research Fund of Affiliated Hospital of Guangdong Medical University (GCC2022010).

Author contributions W. W.: Conceptualization, Methodology, Investigation, Data curation, Writing—original draft, Supervision, Funding acquisition. X. L.: Investigation, Methodology, Data curation, Formal analysis. Z. Z.: Investigation, Data curation, Formal analysis. H. H.: Investigation. C. P.: Investigation. S.Y.: Conceptualization, Methodology, Supervision. JH. Q.: Conceptualization, Funding acquisition, Writing—review & editing, Supervision.

Funding This work was funded by the Guangdong Province's Natural Science Foundation of Basic and Applied Basic Research (2024A1515013013), Competitive Allocation Project of Zhanjiang Municipal Science and Technology Development Special Fund (2021A05055, 2022A01165), and the High-level Talent Initial Scientific Research Fund of Affiliated Hospital of Guangdong Medical University (GCC2022010).

Data availability No datasets were generated or analysed during the current study.

Declarations

Competing interests The authors declare no competing interests.

Ethics approval All animal experiments were approved by the Animal Ethics and Welfare Committee of the Affiliated Hospital of Guangdong Medical University (No. AHGDMU-LAC-B-202304–0027).

References

Chen Y, Lei J, He S. m6A Modification Mediates Mucosal Immune Microenvironment and Therapeutic Response in Inflammatory Bowel Disease. Front Cell Dev Biol. 2021;9:692160.

Cui X, Zhou S, Lin Y. Long non-coding RNA DHRS4 antisense RNA 1 inhibits ectopic endometrial cell proliferation, migration, and invasion in endometriosis by regulating microRNA-139-5p expression. Bioengineered. 2022;13:9792–804.

Ding X, Li D, Li M, Wang H, He Q, Wang Y, Yu H, Tian D, Yu Q. SLC26A3 (DRA) prevents TNF-alpha-induced barrier dysfunction and dextran sulfate sodium-induced acute colitis. Lab Invest. 2018;98:462–76.

Entezari M, Taheriazam A, Orouei S, Fallah S, Sanaei A, Hejazi ES, Kakavand A, Rezaei S, Heidari H, Behroozaghdam M, Daneshi S, Salimimoghadam S, Mirzaei S, Hashemi M, Samarghandian S. LncRNA-miRNA axis in tumor progression and therapy response: An emphasis on molecular interactions and therapeutic interventions. Biomed Pharmacother. 2022;154:113609.

Gao G, Duan Y, Chang F, Zhang T, Huang X, Yu C. METTL14 promotes apoptosis of spinal cord neurons by inducing EEF1A2 m6A methylation in spinal cord injury. Cell Death Discov. 2022;8:15.

GBD 2017 Inflammatory Bowel Disease Collaborators. The global, regional, and national burden of inflammatory bowel disease in 195 countries and territories, 1990–2017: a systematic analysis for the Global Burden of Disease Study 2017. Lancet Gastroenterol Hepatol. 2020;5:17–30.

He RZ, Jiang J, Luo DX. The functions of N6-methyladenosine modification in lncRNAs. Genes Dis. 2020;7:598–605.

Lan Q, Liu PY, Haase J, Bell JL, Hüttelmaier S, Liu T. The Critical Role of RNA m6A Methylation in Cancer. Cancer Res. 2019;79:1285–92.

Li Q, Wen S, Ye W, Zhao S, Liu X. The potential roles of m6A modification in regulating the inflammatory response in microglia. J Neuroinflammation. 2021;18:149.

Li X, Li Y, Wang Y, He X. The m6A demethylase FTO promotes renal epithelial-mesenchymal transition by reducing the m6A modification of lncRNA GAS5. Cytokine. 2022;159:156000.

Lin L, Zhou G, Chen P, Wang Y, Han J, Chen M, He Y, Zhang S. Which long noncoding RNAs and circular RNAs contribute to inflammatory bowel disease? Cell Death Dis. 2020;11:456.

Lu TX, Zheng Z, Zhang L, Sun HL, Bissonnette M, Huang H, He C. A New Model of Spontaneous Colitis in Mice Induced by Deletion of an RNA m6A Methyltransferase Component METTL14 in T Cells. Cell Mol Gastroenterol Hepatol. 2020;10:747–61.

Lu Z, Liu H, Song N, Liang Y, Zhu J, Chen J, Ning Y, Hu J, Fang Y, Teng J, Zou J, Dai Y, Ding X. METTL14 aggravates podocyte injury and glomerulopathy progression through N6-methyladenosine-dependent downregulating of Sirt1. Cell Death Dis. 2021;12:881.

Luo H, Cao G, Luo C, Tan D, Vong CT, Xu Y, Wang S, Lu H, Wang Y, Jing W. Emerging pharmacotherapy for inflammatory bowel diseases. Pharmacol Res. 2022;178:106146.

Luo J, Xu T, Sun K. N6-Methyladenosine RNA Modification in Inflammation: Roles, Mechanisms, and Applications. Front Cell Dev Biol. 2021;9:670711.

Ren T, Qiu Y, Wu W, Feng X, Ye S, Wang Z, Tian T, He Y, Yu C, Zhou Y. Activation of adenosine A3 receptor alleviates TNF-α-induced inflammation through inhibition of the NF-κB signaling pathway in human colonic epithelial cells. Mediators Inflamm. 2014;2014:818251.

Sairenji T, Collins KL, Evans DV. An Update on Inflammatory Bowel Disease. Prim Care. 2017;44:673–92.

Semiz A, Acar OO, Cetin H, Semiz G, Sen A. Suppression of Inflammatory Cytokines Expression with Bitter Melon (Momordica Charantia) in TNBS-instigated Ulcerative Colitis. J Transl Int Med. 2020;8:177–87.

Su T, Liu J, Zhang N, Wang T, Han L, Wang S, Yang M. New insights on the interplays between m6A modifications and microRNA or lncRNA in gastrointestinal cancers. Front Cell Dev Biol. 2023;11:1157797.

Wang JY, Lu AQ. The biological function of m6A reader YTHDF2 and its role in human disease. Cancer Cell Int. 2021;21:109.

Wu J, Deng LJ, Xia YR, Leng RX, Fan YG, Pan HF, Ye DQ. Involvement of N6-methyladenosine modifications of long noncoding RNAs in systemic lupus erythematosus. Mol Immunol. 2022;143:77–84.

Wu W, He Y, Feng X, Ye S, Wang H, Tan W, Yu C, Hu J, Zheng R, Zhou Y. MicroRNA-206 is involved in the pathogenesis of ulcerative colitis via regulation of adenosine A3 receptor. Oncotarget. 2017;8:705–21.

Wu W, Yang H, Li X, Zhou Z, Tan W, Quan JH. METTL14 is Involved in TNF-α-Induced Inflammation in Colorectal Epithelial Cells via Autophagy Modulation. Appl Biochem Biotechnol. 2024 Jun 15. Epub ahead of print.

Xiao L, Zhang Y, Luo Q, Guo C, Chen Z, Lai C. DHRS4-AS1 regulate gastric cancer apoptosis and cell proliferation by destabilizing DHX9 and inhibited the association between DHX9 and ILF3. Cancer Cell Int. 2023;23:304.

Yan F, Zhao W, Xu X, Li C, Li X, Liu S, Shi L, Wu Y. LncRNA DHRS4-AS1 Inhibits the Stemness of NSCLC Cells by Sponging miR-224-3p and Upregulating TP53 and TET1. Front Cell Dev Biol. 2020;8:585251.

Yang L, Wu G, Wu Q, Peng L, Yuan L. METTL3 overexpression aggravates LPS-induced cellular inflammation in mouse intestinal epithelial cells and DSS-induced IBD in mice. Cell Death Discov. 2022;8:62.

Yang X, Zhang S, He C, Xue P, Zhang L, He Z, Zang L, Feng B, Sun J, Zheng M. METTL14 suppresses proliferation and metastasis of colorectal cancer by downregulating oncogenic long non-coding RNA XIST. Mol Cancer. 2020;19:46.

Zeng Z, Jiang M, Li X, Yuan J, Zhang H. Precision medicine in inflammatory bowel disease. Precis Clin Med. 2023;6:pbad033.

Zheng D, Yu L, Wei Z, Xia K, Guo W. N6-Methyladenosine-Related lncRNAs Are Potential Prognostic Biomarkers and Correlated With Tumor Immune Microenvironment in Osteosarcoma. Front Genet. 2022;12:805607.

Zhou H, Yin K, Zhang Y, Tian J, Wang S. The RNA m6A writer METTL14 in cancers: Roles, structures, and applications. Biochim Biophys Acta Rev Cancer. 2021a;1876:188609.

Zhou Y, Li K, Zou X, Hua Z, Wang H, Bian W, Wang H, Chen F, Dai T. LncRNA DHRS4-AS1 ameliorates hepatocellular carcinoma by suppressing proliferation and promoting apoptosis via miR-522-3p/SOCS5 axis. Bioengineered. 2021b;12:10862–77.

Zhuang S, Ma Y, Zeng Y, Lu C, Yang F, Jiang N, Ge J, Ju H, Zhong C, Wang J, Zhang J, Jiang S. METTL14 promotes doxorubicin-induced cardiomyocyte ferroptosis by regulating the KCNQ1OT1-miR-7-5p-TFRC axis. Cell Biol Toxicol. 2023;39:1015–35.

Zong X, Zhao J, Wang H, Lu Z, Wang F, Du H, Wang Y. Mettl3 Deficiency Sustains Long-Chain Fatty Acid Absorption through Suppressing Traf6-Dependent Inflammation Response. J Immunol. 2019;202:567–78.